

SN H0pe: The First Measurement of H0 from a Multiply-Imaged Type Ia Supernova, Discovered by JWST

Massimo Pascale et al. 2024 (arXiv: 2403.18902)

Brenda L. Frye et al. 2024, ApJ, 961, 171

Wenlei Chen et al. 2024 (arXiv: 2403.19029)

J. D. R. Pierel et al. 2024 (arXiv: 2403.18954)

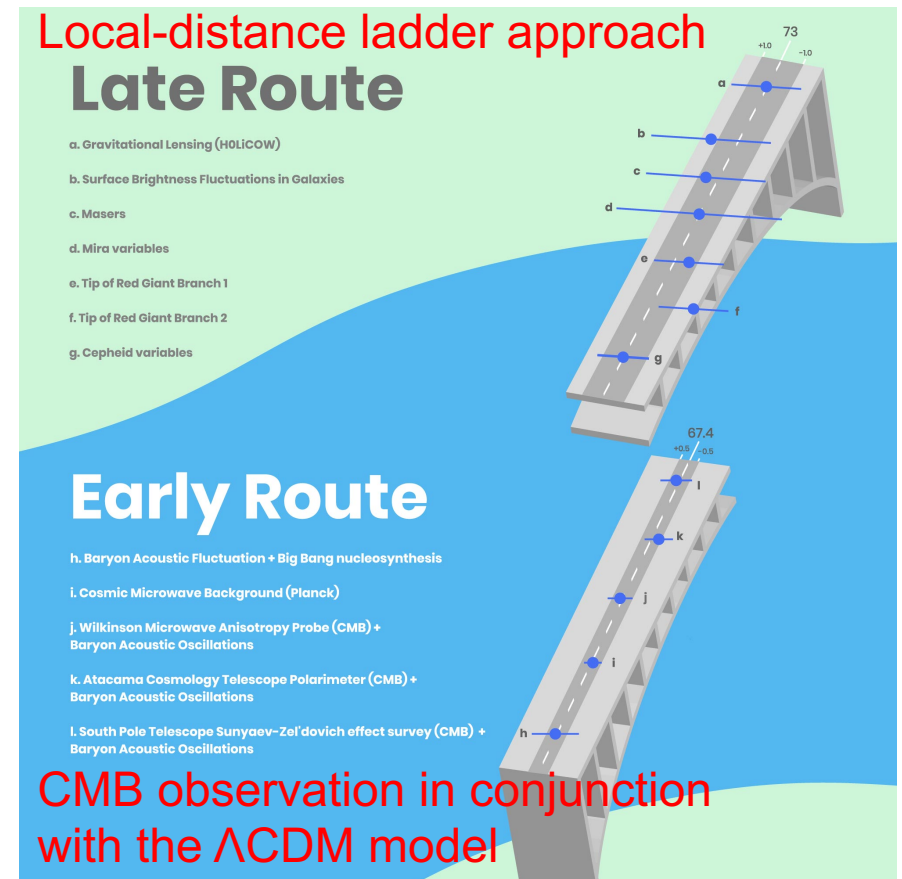
Journal Club @ May. 15

Outline

- Introduction
- Observations
- Time delays Measurements
- Time delay cosmography
- H_0 constraints
- Conclusions

Introduction

- Determination of the current expansion rate of the Universe (the Hubble Constant, H_0) across a wide range of redshifts provides a fundamental test of the standard cosmological model.
- Disagreement between independent measurements of H_0 at early and late times in the Universe ('Hubble tension') raises doubts about the model's reliability.
- For the local distance-ladder, SH0ES team (Riess et al. 2022) yields $H_0 = 73.04 \pm 1.04 \text{ km s}^{-1} \text{ Mpc}^{-1}$
- CMB measurements (Planck Collaboration et al. 2020) from the Planck satellite favor $H_0 = 67.4 \pm 0.6 \text{ km s}^{-1} \text{ Mpc}^{-1}$
- Confirming or resolving the H_0 discrepancy is crucial for fundamental physics



Introduction

- Other independent H_0 measurements

- ‘Tip of the red-giant branch’ (TRGB) yield a range in H_0 of $70\text{--}73 \text{ km s}^{-1} \text{ Mpc}^{-1}$

- The Maser Cosmology Project (MCP, Pesce et al. 2020) combined six maser distances and peculiar velocities to find $H_0 = 73.9 \pm 3.0 \text{ km s}^{-1} \text{ Mpc}^{-1}$

- Strongly gravitationally lensed quasars:

The Time Delay COSMOgraphy (TDCOSMO) collaboration leveraged a joint measurement across seven lensed quasars to find $H_0 = 74.2 \pm 1.6 \text{ km s}^{-1} \text{ Mpc}^{-1}$ assuming power-law mass profiles for the lens and a flat Λ CDM cosmology, and $H_0 = 73.3 \pm 5.8 \text{ km s}^{-1} \text{ Mpc}^{-1}$ using free form mass profiles (Birrer et al. 2020).

- This growing catalog of independent measurements has already provided insights into the Hubble tension, and new measurements at intermediate redshifts $1 < z < 10$ are imperative in elucidating when in cosmic history this discrepancy occurs.

Introduction

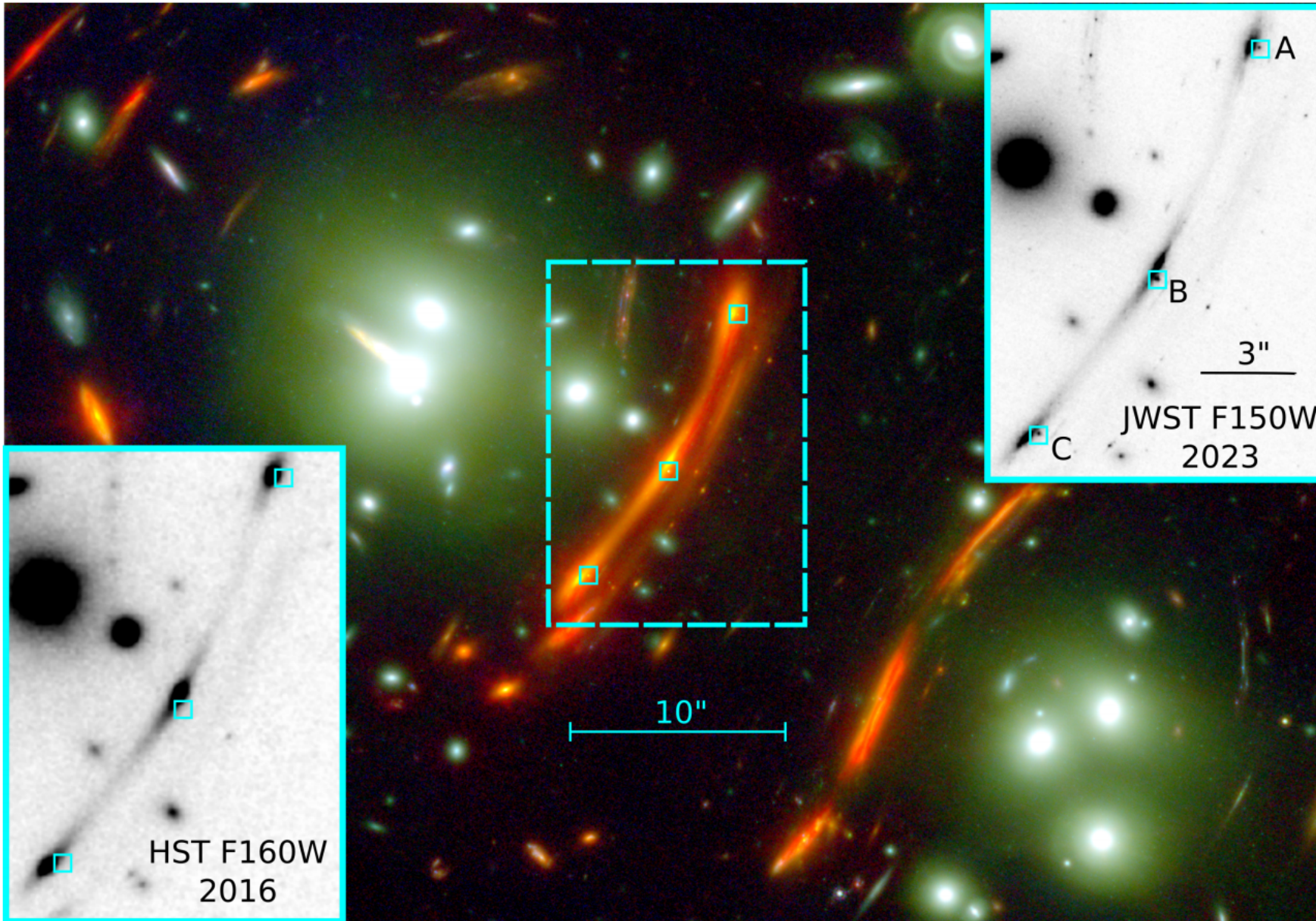
- This work focused on strong gravitational lensing of SNe (Refsdal 1964)
- First realized for SNe for the discovery of ‘SN Refsdal’, a multiply-imaged Type II SN found in the MACS J1149.6+2223 cluster field (Kelly et al. 2015), inferred $H_0 = 64.8^{+4.4}_{-4.3} \text{ km s}^{-1} \text{ Mpc}^{-1}$ or $H_0 = 66.6^{+4.1}_{-3.3} \text{ km s}^{-1} \text{ Mpc}^{-1}$ depending on the set of lens models used.
- After that, multiple other lensed supernova have been observed:
 - Type II SN, such as the $z \sim 3$ SN in the Abell 370 cluster field (Chen et al. 2022)
 - SN Ia,
 - ‘iPTF16geu’ at $z = 0.409$ (Goobaret al. 2017), the first SN Ia to have multiple images observed;
 - ‘SN Zwicky’ at $z = 0.3554$ (Goobar et al. 2023; Pierel et al. 2023); galaxy-scale lenses, whose \sim day-long time delays limited inference of H_0 to $\gtrsim 40\%$ precision
 - ‘SN Requiem’ at $z = 1.95$ (Rodney et al. 2021), galaxy-cluster-scale lens, a nearly decade-long time delay, which will yield a precision measurement of H_0 in 2037 when the SN counterimage is predicted to appear.

Across all of these SNe, SN Refsdal is the only to provide precision H_0 constraints to date.

Introduction

- SN H0pe is a triply-imaged SN Ia discovered in the galaxy-cluster field PLCK G165.7+67.0 ('G165', $z=0.348$). It is a massive lensing galaxy cluster ($M_{\text{tot}}=(2.6 \pm 0.3) \times 10^{14}$ Msun, Frye et al. 2019), that induces a relatively long ~ 100 day time delay between the first and third image, offering only the second-ever opportunity for precision SN time-delay cosmography and the first with a SN Ia.
- This paper presents the first precision measurement of H_0 from time-delay cosmography of a strongly-lensed SN Ia.

Observations



- Discovered on 31 March 2023
- The discovery prompted a JWST disruptive Director's Discretionary Time (DDT) program which acquired two additional epochs of NIRCcam imaging on 22 April 2023 and 9 May 2023.
- The DDT program also acquired JWST/NIRSpec Micro-shutter assembly (MSA) spectra targeting the SN host galaxy and the two brightest SN images.

JWST/NIRCam color image in the central region of G165.

Observations

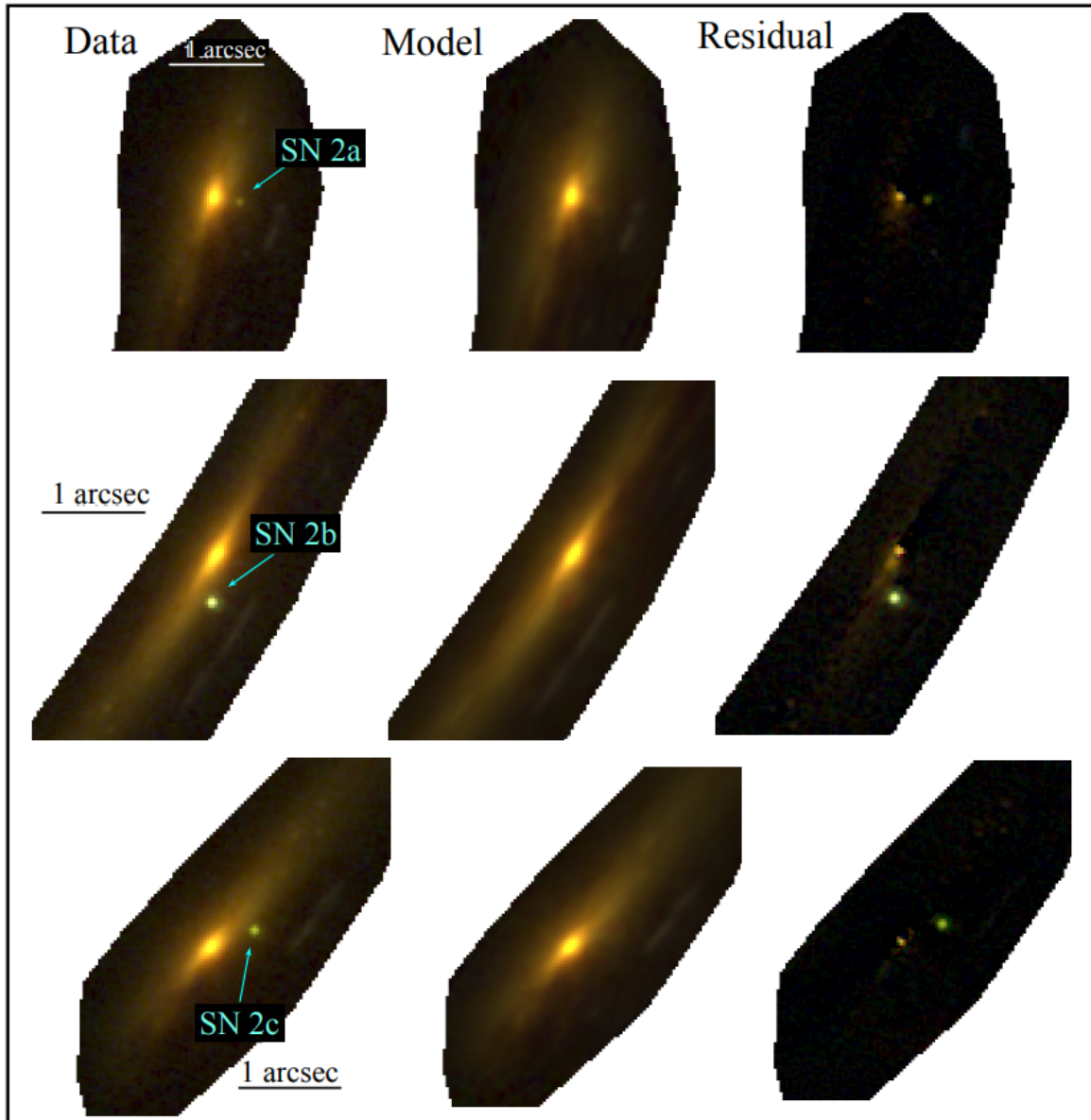


Figure 3. Host light subtraction for Arc 2. Color composite images of epoch 1 using the filters F090W, F150W and F200W as blue, green and red, respectively. Left panels show the original data, middle panels show the surface brightness distribution predicted by our strong lensing total mass model, and right panels show the residuals (i.e. data–model) with the same scaling. Note that the SN is not present in the model, and so it is expected to be present in the residuals. The orientation is the same as in Figure 1.

Observations

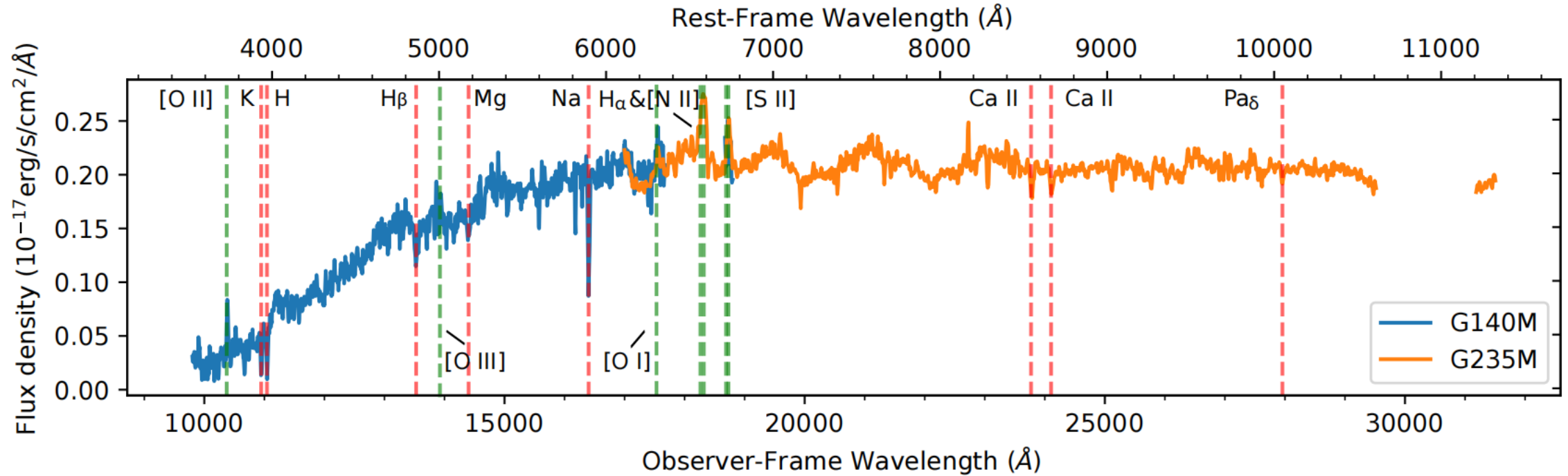


Figure 3. NIRSpec G140M and G235M spectra of the A image of the host-galaxy nucleus. The data are for the single $0''.46$ slitlet containing the nucleus (Figure 1). Vertical lines mark the positions of the detected emission (green) and absorption (red) lines, as listed in Table 1. Wavelengths are marked in the observed frame (bottom) and in the $z = 1.7825$ rest frame (top). The gap in the spectrum near observed $3\ \mu\text{m}$ is from the physical gap between the two NIRSpec detector chips. The spectra and line identifications for Images A and C are also shown by [Frye et al. \(2024\)](#).

Observations

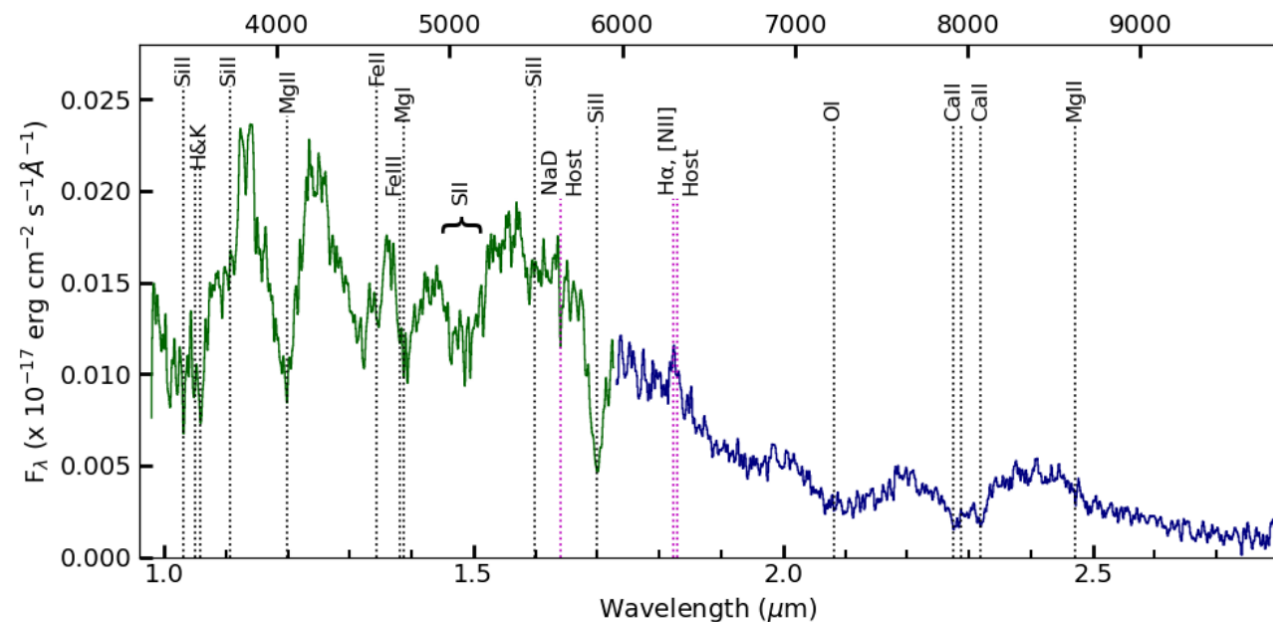
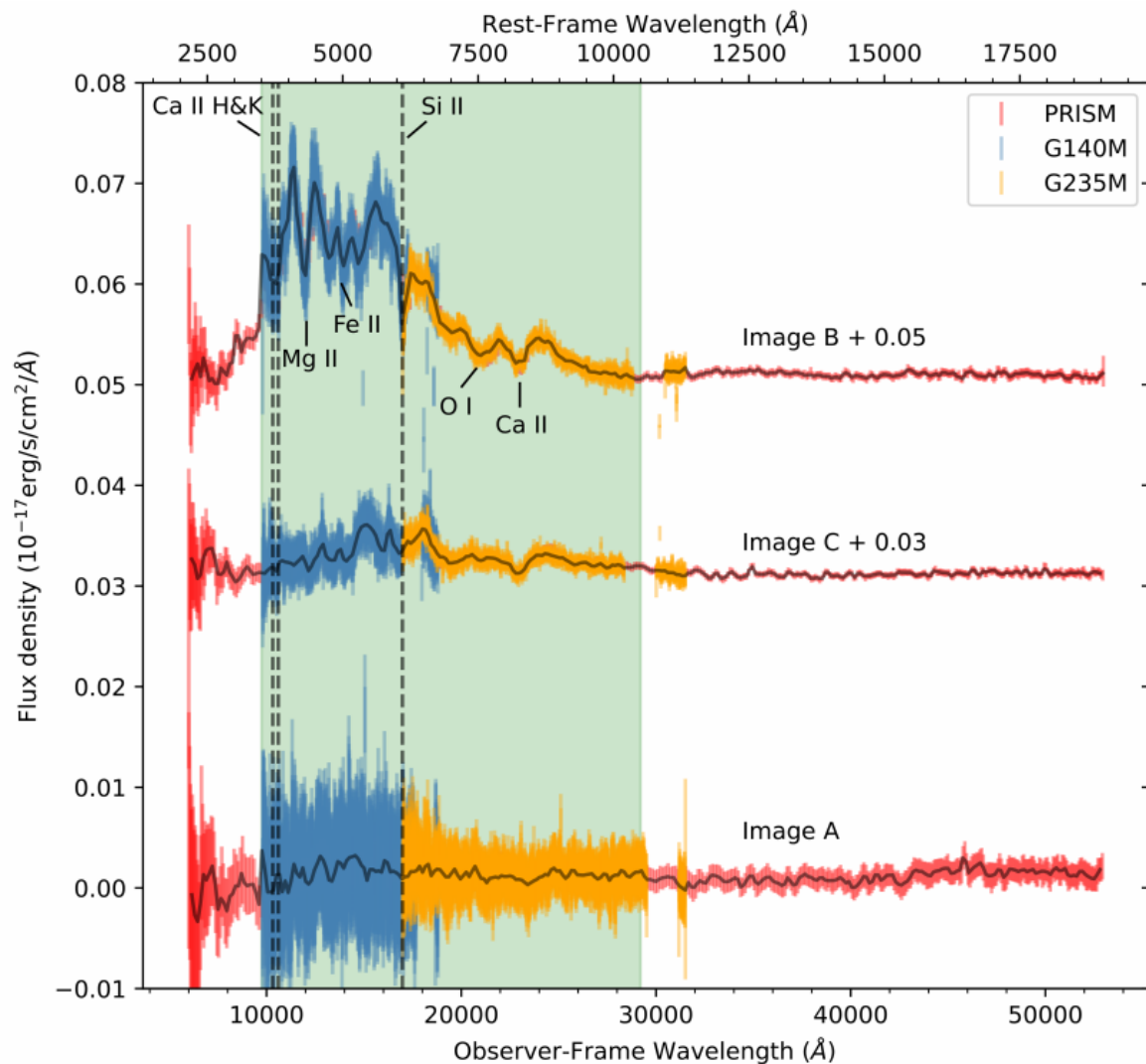
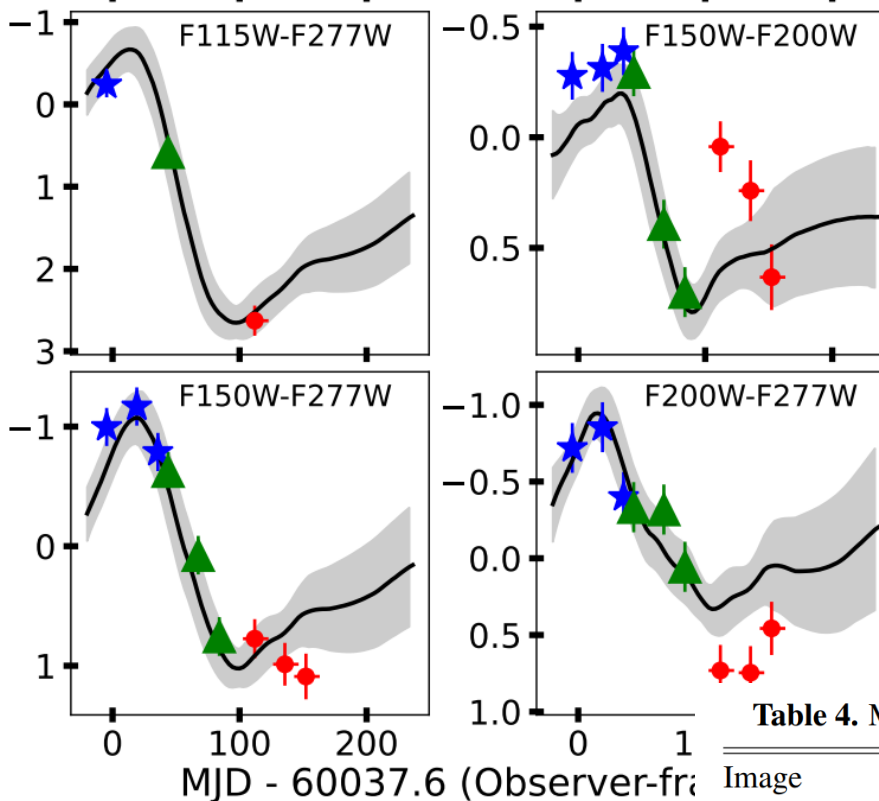
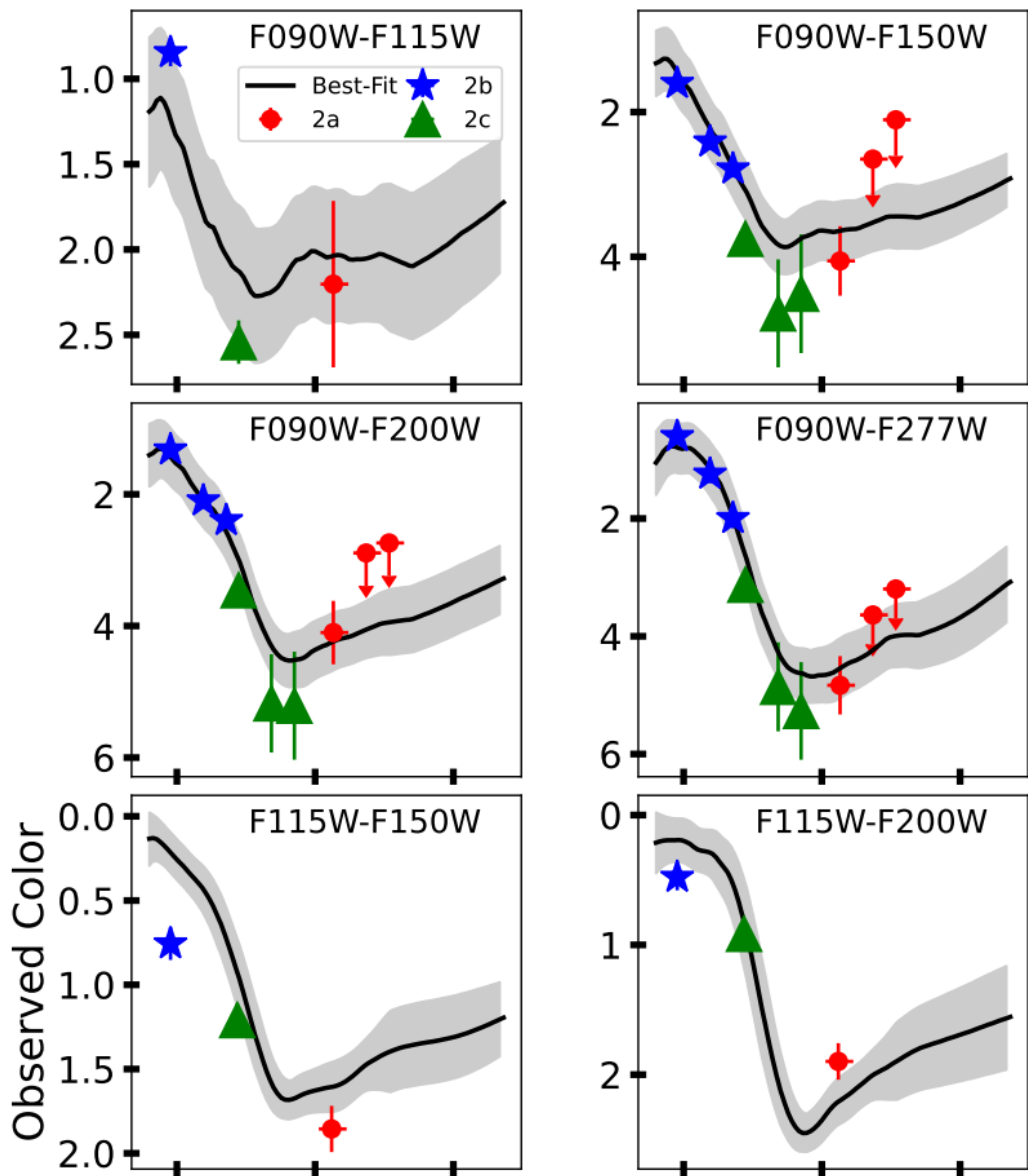


Figure 2. High signal-to-noise NIRSpect spectrum of SN H0pe. The G140M (green) and G235M (blue) grating spectra are shown. Some prominent line features are identified, such as the [Si II] line blueshifted to rest-frame $\sim 6150 \text{ \AA}$ that is a requisite line feature of a Type Ia supernova. A couple of features are also traced to the SN host galaxy, such as NaD, H α , [N II] $\lambda\lambda 6548, 6584$ (magenta dotted-line). The observed wavelength is given on the lower abscissa and the rest wavelength in the frame of the host galaxy is provided on the upper abscissa.

The spectra, taken on 22 April, confirmed the Ia type from the identification of the requisite blueshifted [Si II] $\lambda 6355$ feature, and other absorption-line features commonly found in Type Ia SNe.

Photometric Time delays

With the knowledge that SN H0pe is a SN Ia, the authors leverage the BayeSN SED model (Mandel et al. 2022) to measure time delays with the SNTD Color method.



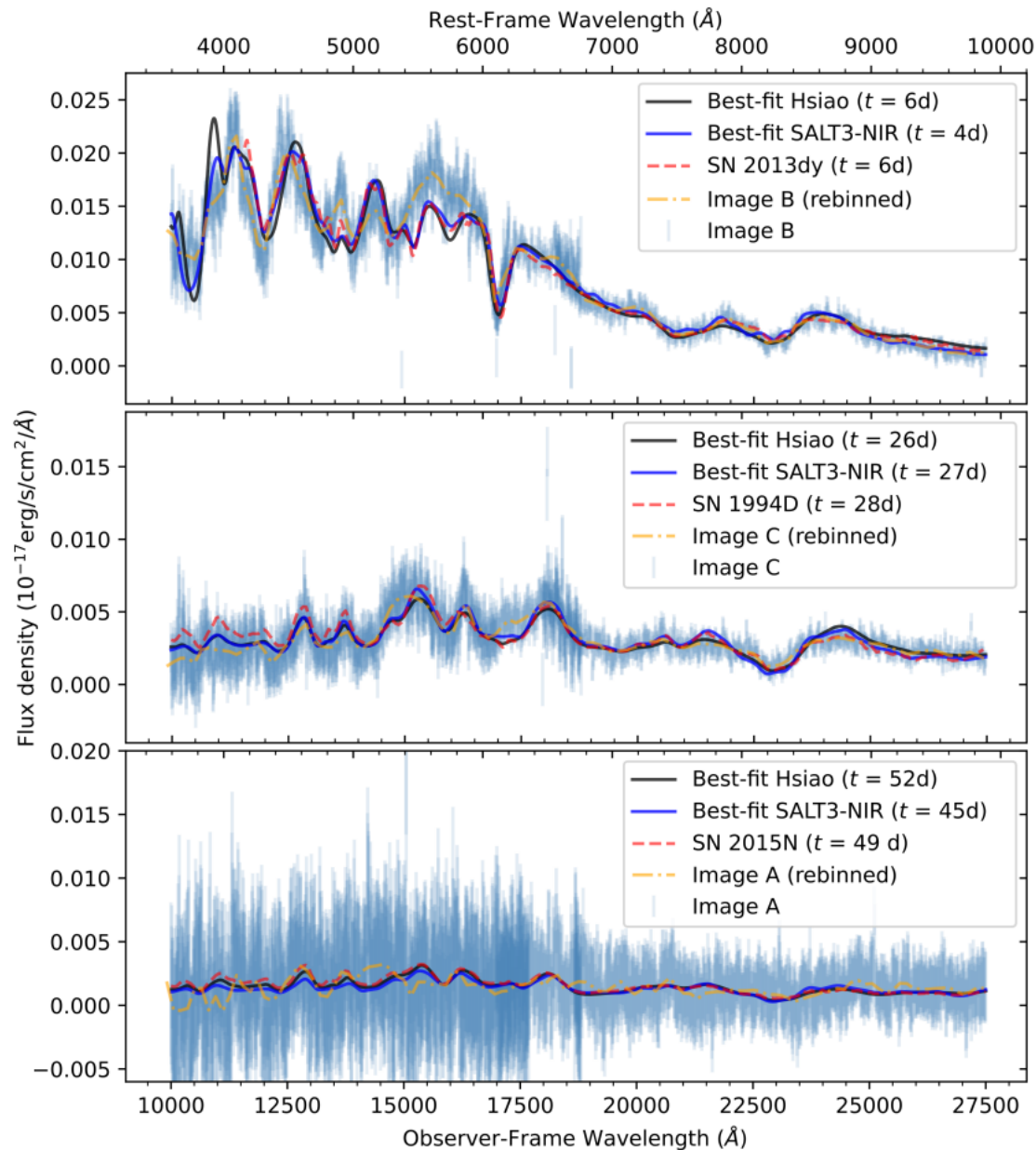
Epoch 1: 8 filters
Epoch 2 & 3: 6 filters

Table 4. Measured time delays and magnifications

Image	$\Delta t (t_i - t_b)$ (Days)	μ
2a	$-116.6^{+10.8}_{-9.3}$	$4.3^{+1.6}_{-1.8}$
2b	—	$7.6^{+3.6}_{-2.6}$
2c	$-48.6^{+3.6}_{-4.0}$	$6.4^{+1.6}_{-1.5}$

Figure 4. Reconstructed color curves for SN H0pe, after applying the best-fit time delays. The vertical error bars are the photometric precision, while the horizontal error bars are the 16th and 84th percentiles simulation recovery time-delay posterior for images 2a and 2c (see Table 5), and t_{pk} for image 2b. The grey shaded region is uncertainty on the best-fit model from the SNTD Color method (black solid).

Spectroscopic Time delays



Straightforward spectroscopic SN Ia template fitting to determine the phases between images

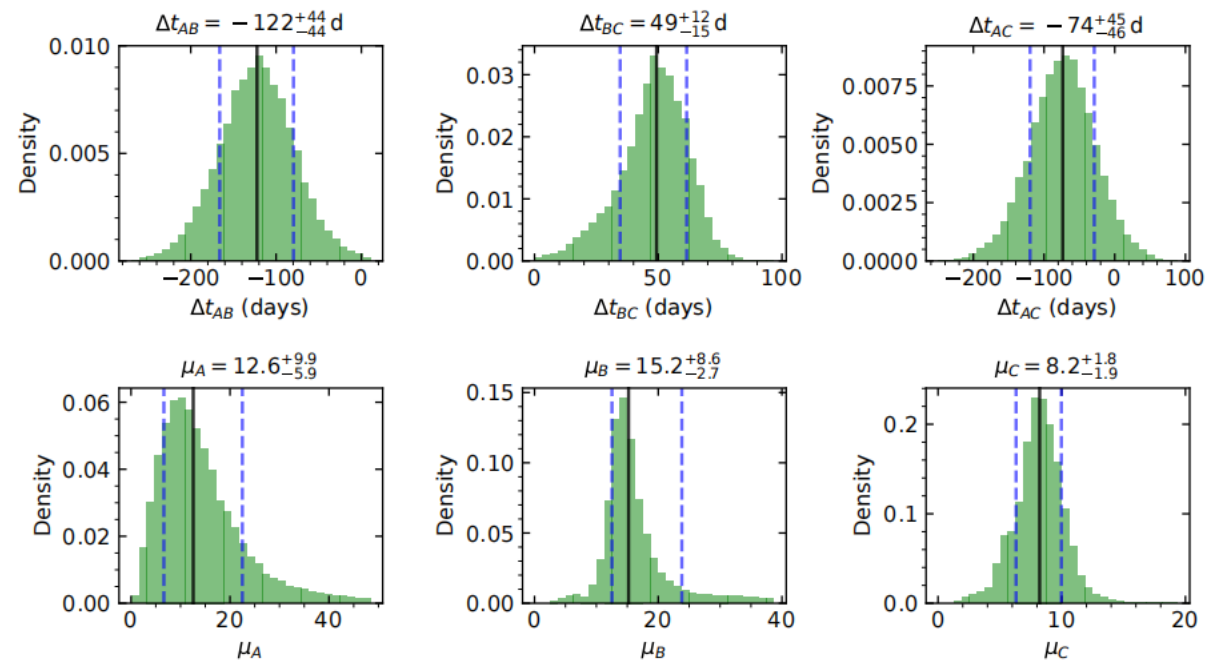


Figure 10. Posterior probability densities of the relative time delays and the macro lens magnifications between SN H0pe's images. Histograms show values derived from the Hsiao07 templates. The distributions integrate the uncertainty from the MCMC fitting with systematic uncertainties, estimated from the model fitting of nearby SN Ia spectra and from the simulated SN Ia spectra. The uncertainties take into account the impacts of microlensing and millilensing effects.

Time delay cosmography

For an individual source at angular position β with a corresponding lensed image observed at angular position θ , the time delay can be expressed as:

$$\Delta t(\theta) = \underbrace{\frac{1 + z_l}{c} \frac{D_l D_s}{D_{ls}}}_{\text{'time delay distance'}} \left[\frac{1}{2} (\theta - \beta)^2 - \psi(\theta) \right]$$

z_l is the redshift of the lensing cluster

$\psi(\theta)$ is the lensing potential at the observed image position θ , and

D_l , D_s , and D_{ls} are the angular diameter distances to the lens, the source, and between the lens and source respectively.

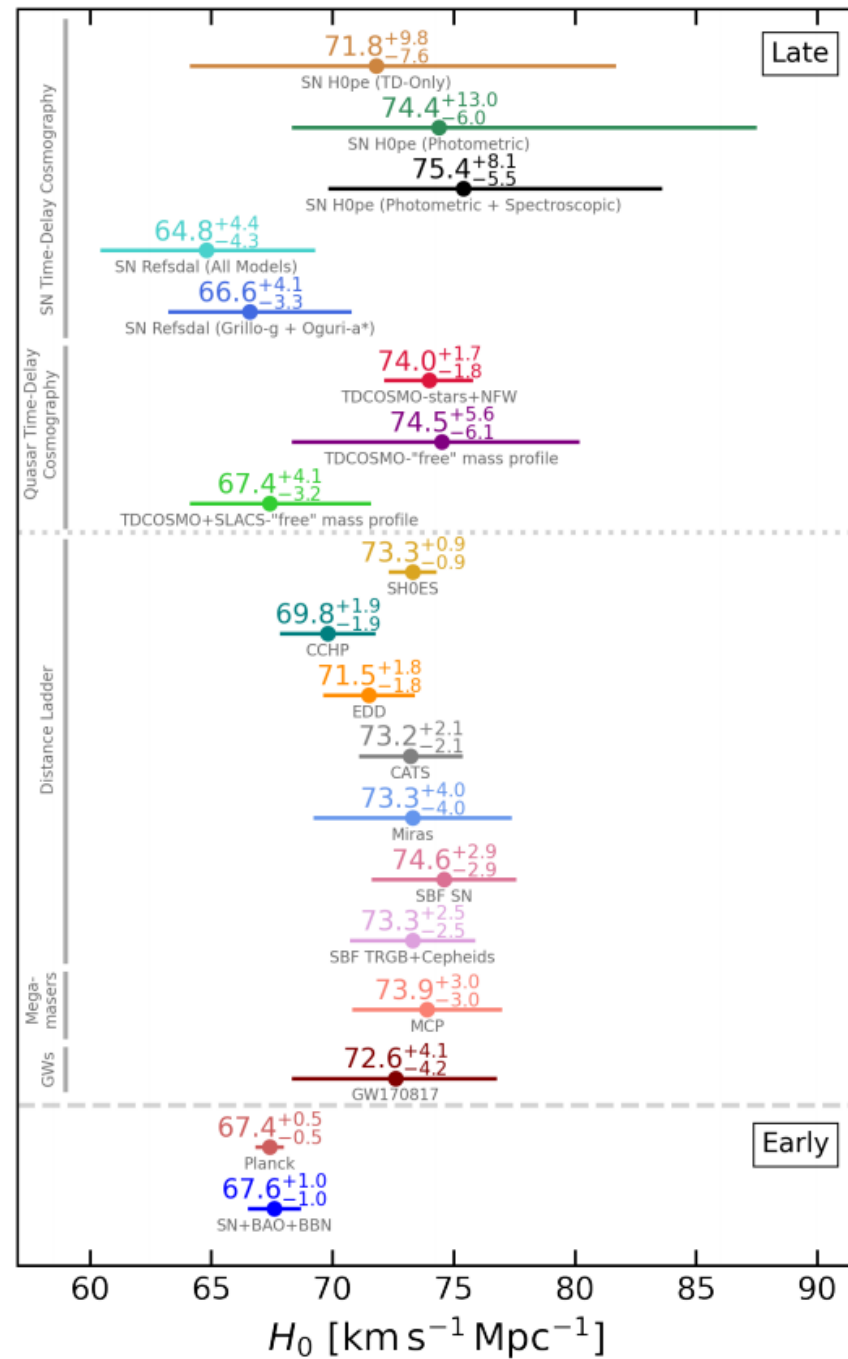
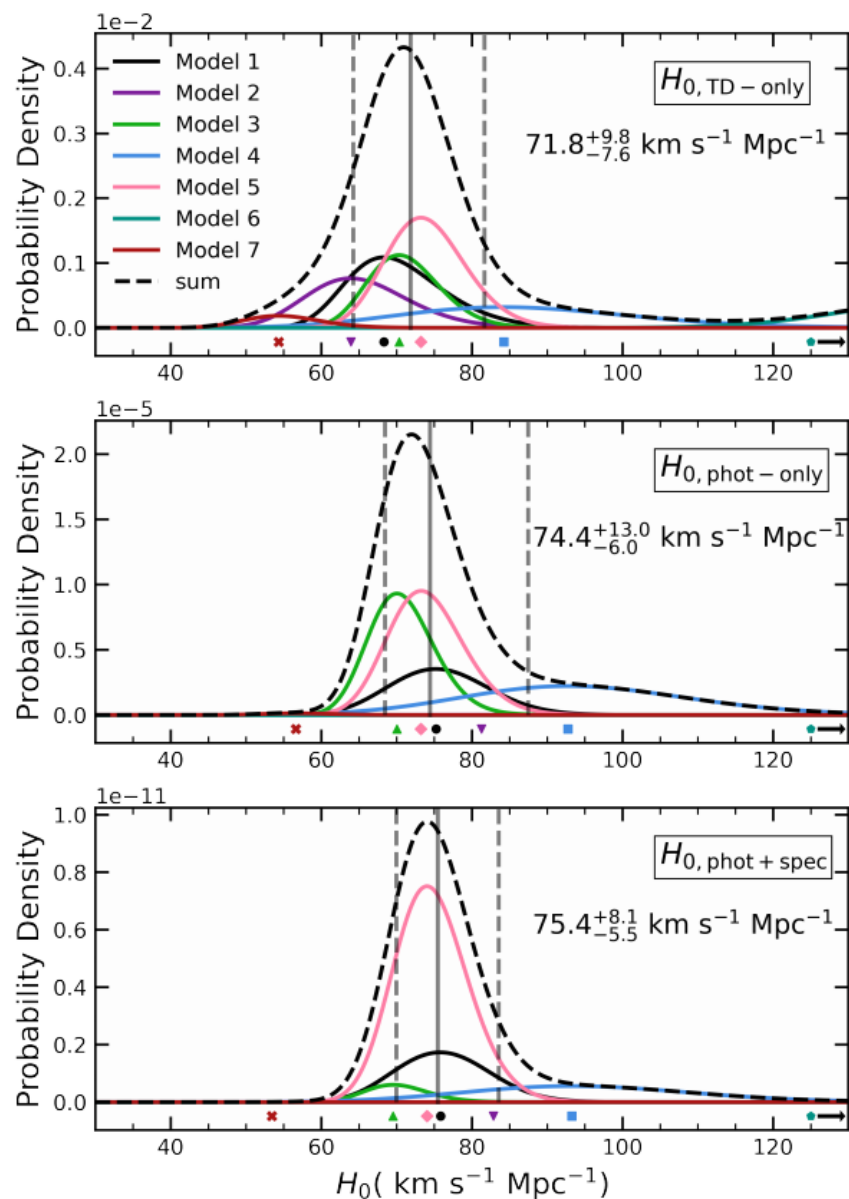
7 different teams constructed independent lens models with the same input constraints:

- 21 image systems, five of them with spectroscopic redshifts
- 161 cluster member galaxies with positions, F200W brightnesses, and morphological parameters

Broadly split into two categories:

- Parametric models (models 1, 2, 3), assume the mass distribution is entirely characterized as the superposition of analytic profiles.
- Non-parametric models (models 4 and 6), on the other hand, make fewer assumptions on the profile of the cluster-scale dark matter, and allow a flexible grid to describe the mass distribution

H0 constraints



Conclusions

- The James Webb Space Telescope (JWST) Near InfraRed Camera (NIRCam) imaging in the field of the galaxy cluster PLCK G165.7+67.0 ($z = 0.35$) uncovered a Type Ia supernova (SN Ia) at $z = 1.78$, called “SN H0pe.”
- SN H0pe is only the second opportunity for precision SN time delay cosmography.
- They measured the probability distribution of H_0 by comparing the photometrically and spectroscopically measured time delays and magnifications to those predicted by seven independently created lens models, inferring $H_0 = 75.4^{+8.1}_{-5.5} \text{ km s}^{-1} \text{ Mpc}^{-1}$
- This is the first precision measurement of H_0 from a multiply-imaged SN Ia, and provides a measurement in a rarely utilized redshift regime.
- This result agrees with other local universe measurements, yet exceeds the value of H_0 derived from the early Universe with $\gtrsim 90\%$ confidence, increasing evidence of the Hubble tension.
- Upcoming surveys from the Vera C. Rubin and Nancy Grace Roman observatories as well as continuing JWST programs will increase the sample of cluster-lensed SNe, which promises to ultimately drive H_0 constraints down to percent-level precision.